7. Sellors, J. W., Nieminen, P., Vesterinen, E. and Paavonen, J., Observer variability in the scoring of colpophotographs. *Obstet. Gynecol.*, 1990, **76**, 1006–1008.
8. Bhatla, N. (ed.), *Jeffcoate's Principles of Gynaecology*, Arnold Publishers, London, 2001.
9. Shastri, S. S. *et al.*, Concurrent evaluation of visual, cytological and HPV testing as screening method for the early detection of cervical neoplasia in Mumbai, India. *Bull. WHO*, 2005, **83**, 186–194.
10. Benedet, J. L., Matisic, J. P. and Bertrand, M. A., The quality of community colposcopic practice. *Obstet. Gynecol.*, 2004, **103**, 92–100.
11. Bharani, B. and Phatak, S., Role of colposcopy in evaluation of lower female genital tract in 175 symptomatic women. *J. Obstet. Gynecol. India*, 2004, **54**, 372–375.

ACKNOWLEDGEMENTS. We are grateful to Dr Neerja Bhatla, AIIMS, New Delhi, and Dr U. Manaktala, MAMC, New Delhi, for their critical comments and suggestions. We are also grateful to Dr M. Sant and Dr A. Lele and the postgraduate students of the Medical College, Jabalpur, for support, and Arvind Kavishwar, RMRCT, Jabalpur, for help in data analysis.

Received 7 October 2007; revised accepted 18 December 2008

Particle field imaging using digital in-line holography

Vijay Raj Singh[1], Gopalkrishna Hegde[2,*] and Anand Asundi[1]

[1]School of Mechanical and Aerospace Engineering, Nanyang Technological University, Singapore 639798
[2]Department of Aerospace Engineering, Indian Institute of Science, Bangalore 560 012, India

Digital holography is the direct recording of holograms using a CCD camera and is an alternative to the use of a film or a plate. In this communication in-line digital holographic microscopy has been explored for its application in particle imaging in 3D. Holograms of particles of about 10 μm size have been digitally reconstructed. Digital focusing was done to image the particles in different planes along the depth of focus. Digital holographic particle imaging results were compared with conventional optical microscope imaging. A methodology for dynamic analysis of microparticles in 3D using in-line digital holography has been proposed.

Keywords: CCD camera, digital holography, holograms, in-line geometry, particle imaging.

DIGITAL holography (DH) is a rapidly growing opto-digital method for imaging, microscopy and metrology[1–10]. In DH, the hologram which is the interference of object and reference waves is recorded in digital form using CCD or CMOS sensors and then numerically reconstructed on the computer. With recent developments in mega-pixel CCD cameras and the fast, efficient reconstruction algorithm, it is now possible to record digital holograms in real time. Use of fast computers in numerical reconstruction makes DH more flexible in terms of hologram processing. The ability of numerical evaluation of both amplitude and phase information is its main advantage over other optical imaging methods. There is no wet chemical process and other time-consuming procedures in DH. Its diverse applications in areas such as microscopy[4], micro-particles imaging[6], 3D imaging[7], interferometry[8], MEMS characterization[9,10], shape measurements[11], particle image velocimetry[12] and in biology[13] are well known. The limited pixel size of the commercially available digital detectors restricts the angle between the object and reference beams to few degrees for hologram recording. Thus in-line geometry proposed by Gabor[1] becomes the preferred choice for digital holography. Also, in-line DH makes efficient use of full sensor area for hologram recording in comparison to off-axis geometry. The main problem with in-line geometry is the overlapping of zero-order and twin image waves with the real-image wave during reconstruction process. Various digital methods have been proposed to suppress these unwanted waves[14,15]. Typical in-line DH applications have also been reported[16,17]. Many such applications are also being explored.

In many situations involving particle fields there is an urgent need to develop optical techniques to measure instantaneous 3D distribution of particles dispersed in a flow. Various optical techniques are developed for instantaneous 3D measurement of particle distribution[18], including stereoscopic particle tracking[19], defocusing digital particle image velocimetry[20], forward scattering particle image velocimetry[21], and holographic techniques such as holographic particle image velocimetry[22–24]. These techniques have limitations either with volume size or particle density or the need for multiple exposure. However, in recent years DH has shown its capability in providing high-resolution, instantaneous measurements of a large number of particles in a 3D volume[7,13,18]. In-line DH for particle imaging has the potential for the measurement of size, position and velocity of particles distributed in 3D. The advantage with in-line DH is that full CCD sensor area is utilized for real-image reconstruction of the objects. The aim of this communication is to demonstrate that selective numerical reconstruction of the hologram in different planes is helpful in visualizing micro-particles along the flow field. A simple digital focusing method to eliminate the defocused particles and display a plane containing only the in-focus particles of the image is proposed. Then, a comparative study of particle imaging using digital in-line holographic microscopy and conventional optical microscopy is presented. Furthermore, only a single holo-

*For correspondence. (e-mail: hegopal@aero.iisc.ernet.in)

gram is necessary to display the particles in different planes along the depth of focus and no other curve-fitting or processing is required. The methodology for dynamic analysis of micro-particles in 3D using in-line DH will be presented later in the communication.

So far, various optical geometries have been proposed for particle analysis using DH[6,16,25]. The simplest and most common optical system for particle analysis is using the collimating laser beam; here a collimated beam is used to shine the particle field distribution. The limitation of such geometry arises because of the poor resolution of the CCD, that restricts the size of particles to be measured. The experimental set-up used is shown in Figure 1 *a*. A 0.532 μm frequency-doubled, spatially filtered collimated Nd–YAG cw laser beam was used to illuminate a 4 mm thick glass slide, which has few micro-particles of sizes ~10 μm on either face. Fresnel hologram was recorded on a CCD placed at distances of 64 and 68 mm from the faces of the slide. The CCD (DFK 41BF02) had 1280×960 square pixels of size 6 μm. A typical digitally recorded hologram of micro-particles in 3D is shown in Figure 1 *b*.

Recent developments in reconstruction algorithm and CCD cameras permit efficient digital holographic reconstruction and quantitative evaluation in real time. The two most common methods used for numerical reconstruction of DH are the Fourier transform (FT) and convolution (CV) methods. In FT method the reconstructed wavefield is Fourier transform of the product of the DH with the complex reference wave and impulse response function. The reconstructed wavefield is defined as:

$$U(x,y) = \Im\{H(\xi,\eta)R(\xi,\eta)g(\xi,\eta)\}\,.$$

Here $H(\xi, \eta)$ is the hologram, $R(\xi, \eta)$ the reconstruction wave and $g(\xi, \eta)$ the impulse response of coherent optical system.

In the FT method of reconstruction, the pixel size of the numerically reconstructed image varies with the reconstruction distance d and is given by:

$$\Delta x = \frac{\lambda d}{M\Delta\xi}, \quad \Delta y = \frac{\lambda d}{N\Delta\eta},$$

where λ is the wavelength used, $\Delta\xi$ and $\Delta\eta$ are the pixel size, and M, N are pixel numbers.

In the CV method, the Fourier transform of the product of the digital hologram and the reference wave is multiplied by the transfer function of the coherent optical system at the reconstruction distance. The reconstructed object wave is then the inverse Fourier transform of this product. In convolution approach of reconstruction, the reconstructed wave is defined as:

$$U(x,y) = [H(\xi,\eta)R(\xi,\eta)] \otimes [g(\xi,\eta)].$$

Here $\otimes$ indicates a two-dimensional convolution. The reconstructed wavefield can be calculated using the convolution theorem as:

$$U(x,y) = \Im^{-1}[\Im\{H(\xi,\eta)R(\xi,\eta)\}\Im\{g(\xi,\eta)\}].$$

The pixel size of the reconstructed image by the CV method is the same as that of the CCD and does not vary with reconstruction distance, i.e. $\Delta x = \Delta\xi$ and $\Delta y = \Delta\eta$.

In the FT method, the magnification of the reconstructed image varies with the reconstruction distance[2], while it remains constant and equal to the pixel size of CCD sensor in the CV method. The FT method can also be used for objects larger than the CCD array size, but the CV method is used only for small objects. We used the CV method for reconstruction.

Figure 2 shows the coordinate system of recording and reconstruction in DH. A collimating laser beam illuminates the particle field, and the hologram formed due to the interference of the directly transmitted light and the light diffracted the particles is recorded using a CCD sensor. Let (x, y) be the object plane and (ξ, η) the hologram plane. The object wave $O(\xi, \eta)$ at the hologram plane is defined as the convolution of amplitude transmittance of the particle $A_0(x, y)$ with the impulse response of the coherent optical system and can be written as

$$O(\xi,\eta) = \frac{\exp(ikd)}{i\lambda d}\iint A_0(x,y) \exp\left[\frac{ik}{2d}\{(\xi-x)^2+(\eta-y)^2\}\right]dxdy, \qquad (1)$$

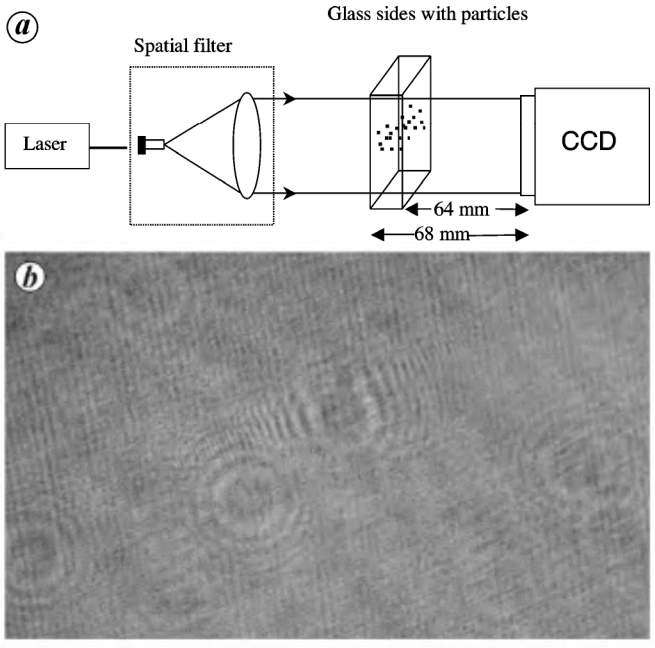

Figure 1. ***a***, Digital in-line holography experimental set-up using collimated laser beam. ***b***, Typical digital in-line hologram of particles.

where $k = 2\pi/\lambda$ is the wave number and d the recording distance.

The interference between the object wave $O(\xi, \eta)$ and plane reference wave $R(\xi, \eta)$ is recorded on the hologram plane (ξ, η). The complex amplitude of the interference pattern at the hologram plane is

$$U(\xi,\eta) = O(\xi,\eta) + R(\xi,\eta) . \quad (2)$$

The CCD sensor records this interference pattern in the form of intensity distribution $H(\xi,\eta) = U(\xi,\eta)U^*(\xi,\eta)$, called a digital hologram, which is stored in the computer.

Thus,

$$H(\xi,\eta) = |O(\xi,\eta)|^2 + |R(\xi,\eta)|^2 + O(\xi,\eta)R^*(\xi,\eta) + O^*(\xi,\eta)R(\xi,\eta), \quad (3)$$

In the reconstruction step, the hologram is multiplied by a reconstruction wave (R') and the reconstructed complex wave field at a distance d' is obtained using the Fresnel's diffraction integral. The numerical reconstruction process was performed using the CV method. The reconstructed wave field can be written as:

$$U(x, y, d') = \{H(\xi,\eta)R'(\xi,\eta)\} \otimes \{g(\xi,\eta)\}, \quad (4)$$

where $g(\xi, \eta)$ is the impulse response of coherent optical system at distance d'.

To reconstruct the real image of the particles, the reconstruction wave should be an exact replica of the complex conjugate of the reference wave ($R' = R^*$). Figure 3 shows the amplitude images at reconstruction distances of 64 and 68 mm using the CV method. When the reconstruction distance was changed to the second plane of the object, the object plane at the first distance is defocused and disappeared in the reconstructed hologram. This is done using a single recorded hologram. In the reconstructed image the bright background is because of the direct wave, and the out-of-focus images of particles appear as hollow circles in the reconstructed images. Also, at the reconstruction distance $d' = d$, the amplitude of the wavefront is a maximum. Since the pixel size of the reconstructed image remains constant with reconstruction distance and is equal to the pixel size of the CCD sensor, the size of the objects can be determined numerically by counting the number of pixels of the reconstructed images.

However, contributions from the reference wave and the conjugate image wave degrade the quality of the reconstructed image. In addition, for a 3D distribution of particles, the defocused images of particles lying outside the focus plane also appear in the final reconstructed image. A method to improve the quality of reconstructed images by sectioning of amplitude images has already been proposed[26]. The same approach has been extended for particle imaging in 3D.

Digital particle holographic system was compared with conventional optical microscopic system. Copolymer micro-spheres of size about 8–10 μm were stuck on a thin glass side. The optical microscopic image of the distribution of particles on the slide is shown in Figure 4 *a*; the magnification of the optical microscope was 10X. Digital in-line hologram of same particle field distribution was recorded, and the numerically reconstructed amplitude image of the particle field is shown in Figure 4 *b*. The effect of out-of-focus twin image appears as circular fringes, which are significantly smaller. The amplitude image by digital particle holography shows a good comparison with the optical microscopic image.

Digital focusing method developed to reconstruct the amplitude images has been extended to particle imaging

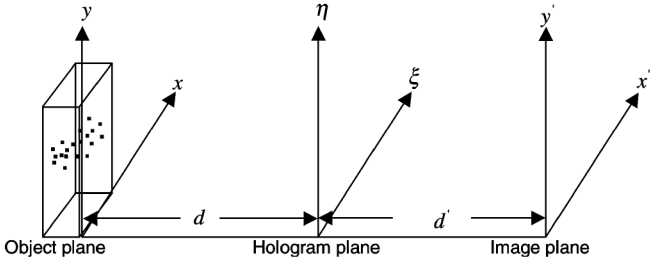

Figure 2. Coordinate system for recording and reconstruction of digital hologram.

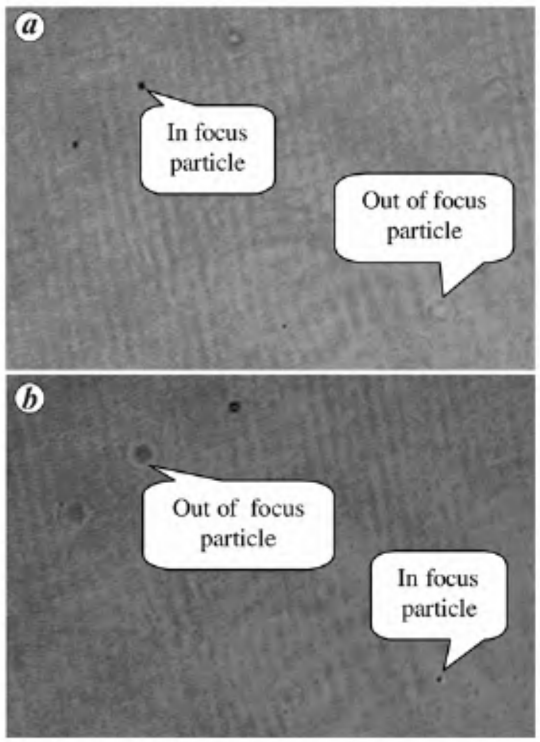

Figure 3. Numerically reconstructed amplitude images of particles (***a***) front side and (***b***) backside of the glass plate.

in 3D. To show the capability of DH for 3D imaging of micro-particles, two thin glass slides were placed at 440 μm apart. Micro-particles of size about 8–10 μm were put on both the slides, as shown in Figure 5 *a*. The optical microscopic images of the particles on both the slides are shown in Figure 5 *b*. The two images were recorded by mechanical focusing of the microscopic objective on each slide.

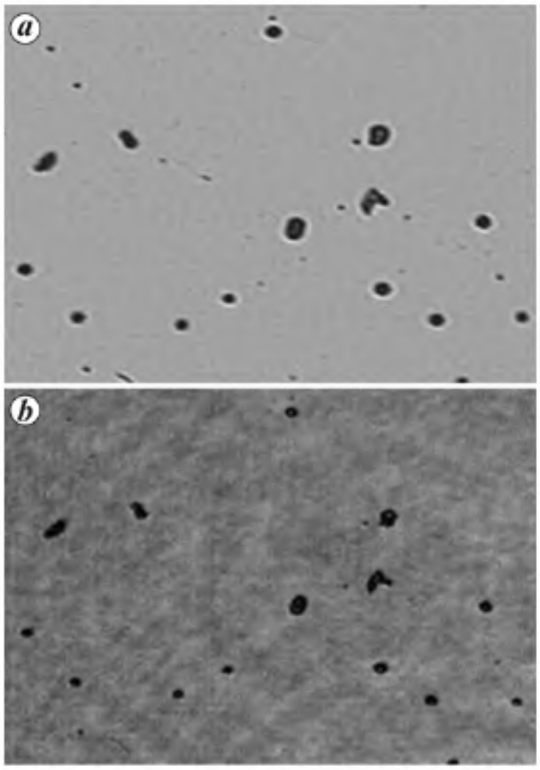

Figure 4. *a*, Optical microscopic image. *b*, Reconstructed digital holographic amplitude image.

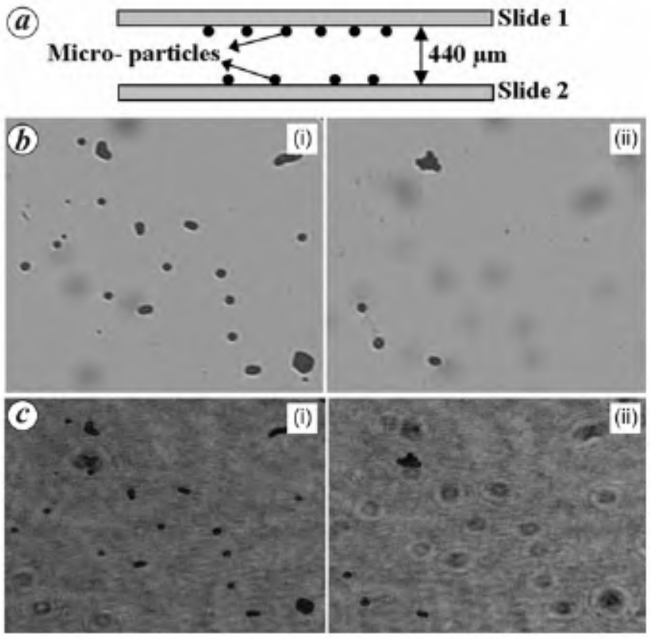

Figure 5. *a*, Micro-particles placed in two different planes. *b*, Optical microscope images of micro-particles on (i) slide 1, and (ii) slide 2. *c*, Numerically reconstructed images of micro-particles on (i) slide 1, and (ii) slide 2.

The same slides were put into the in-line DH set-up as explained earlier and a single hologram was recorded using the CCD sensor. This recorded hologram contains all the information that is required to reconstruct the whole 3D image of particles. The numerically focused images on the corresponding planes are shown in Figure 5 *c*. The advantage with DH is that a single hologram can provide all 3D sections of the particle images. It can be clearly seen that all the particles which are visible in the optical microscopic images are clearly resolved in numerical reconstruction. Thus a single hologram provides the high-resolution images of particles in whole 3D volume. However, in conventional optical microscopy many images have to be recorded for particles in as many planes.

Particle analysis using collimated wave DH is limited for the study of larger size of particles, along with significantly large depth of focus. The pixel size of available CCD sensor restricts the resolution of the system, and limited numerical aperture results in poor depth resolution. To improve the in-line digital holographic system capability, lensless digital holographic microscopy (LDHM)[27,28] system has been explored for micro-particles analysis.

The experimental arrangement for digital in-line LDHM is shown in Figure 6. Micro-particles imaging in 3D was performed using the LDHM system. The capability of the system has been explored for the measurement of location and size of micro-particles in 3D. Copolymer microspheres of size 8–10 μm have been studied using LDHM. The particles were flowing in water contained in a cuvette of size 10×10 mm. CW laser beam of wavelength 0.405 μm was expanded using a microscope objective of 60X and the sample was placed in the path of the highly diverging, spatially filtered beam coming out of the pinhole.

The hologram of the particle system was recorded using the CCD sensor of 4.65×4.65 μm pixel size. The CCD sensor was placed at the distance of 35 mm from the pinhole and the sample was placed in between. The recorded hologram was stored in the computer and the numerical reconstruction process was performed using

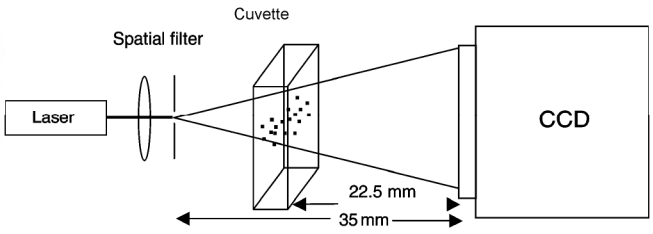

Figure 6. Experimental set-up for digital in-line holographic particle imaging.

converging reference wave. The reconstructed amplitude images of the particle field at distances 22.55 and 23.1 mm from the hologram plane are shown in Figure 7 *a* and *b* respectively. Reconstruction of the hologram was performed by subtracting the reference wave (without sample) from the hologram. This kind of hologram preprocessing is used to suppress the zero-order term. The use of highly diverging wave[3] improves the system resolution in 3D.

Let us consider depth measurement using Z profile. Here the depth of focus of the system depends on the system NA and is defined as, $\Delta z \geq \lambda/2\ (\mathrm{NA})^2$. The depth location of the particle in 3D space can be identified by using the average intensity value of the pixels displaying the particle amplitude image. The position where the intensity value becomes maximum represents the particle position in 3D. The average intensity depth profile of the encircled particle in Figure 7 *a* is shown in Figure 8. The intensity plot of particle image along depth was used to calculate the location of the particle. In the present experiment the intensity peak shows the depth resolution about five times the particle diameter. Thus the LDHM system is a better option for the study of smaller size particles with higher depth resolution compared to collimated wave geometry, because of larger NA.

To determine the size of the particles, the intensity value of the reconstructing pixels can be used for measurements along X and Y directions. The particle shown in Figure 7 *a* is considered for the size measurement. The intensity profile is along the X and Y directions are shown in Figure 9 *a* and *b* respectively. The size of the particle can be determined by calculating the number of pixels, and multiplying the reconstructed pixel size by the number of pixels obtained from the peak of the curve.

The effect of magnification of the particles considered in different locations in 3D can change the number of reconstructed pixels showing the particle image. This effect can be seen in Figure 10, which shows the X and Y profiles of the particle 1 of Figure 7 *b*. It can be clearly seen that the number of pixels is larger in comparison to Figure 9. Thus incorporation of magnification effect along with pixel size is required for the study of size-distribution analysis from reconstructed images at different depths.

Dynamic analysis of micro-particles was performed using LDHM. To study the dynamics of micro-particles flowing in any fluid or gas medium, first the sequence of holograms has to be recorded corresponding to the dynamic changes. The reconstruction process is then performed to analyse the particle field. One simple method is to reconstruct the holograms at different depths and visualize the particle behaviour corresponding to different frames. Two methodologies are presented here for the dynamic micro-particles analysis. The experiment has been performed with polymer spheres suspended in water held in a cuvette. Three holograms were recorded at an interval of 1 s each using the CCD sensor. The holograms were then reconstructed for dynamic analysis of the particles in 3D.

The dynamic analysis in 3D by holograms addition, the recorded holograms were added first and then the reconstruction process was performed. The dynamic behaviour of particles can be studied during the reconstruction of the final hologram (addition of holograms). To explain this method, three holograms were recorded of the microspheres flowing in water. The experimental arrangement shown in Figure 6 was used for the recording process. The reconstructed images of the particles corresponding to each hologram (recorded at an interval 1 s each) are shown in Figure 11 *a–c* respectively (reconstruction distance is 21.79 mm). Two micro-spheres can be seen in each figure, and their pixel positions have been changed in each frame representing the dynamic flow. The recorded holograms were added first and then the reconstruction performed for the sum of the holograms. The reconstructed image of the added holograms is shown in Figure 11 *d*. The reconstructed particle image can be seen in a single reconstructed frame, which clearly shows the dynamic behaviour of the particle motion.

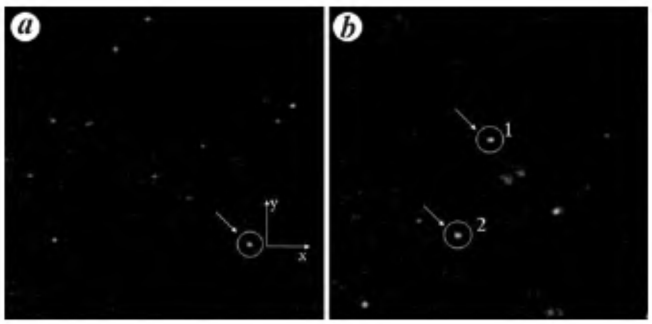

Figure 7. Reconstructed intensity images showing micro-particle field distribution in different planes.

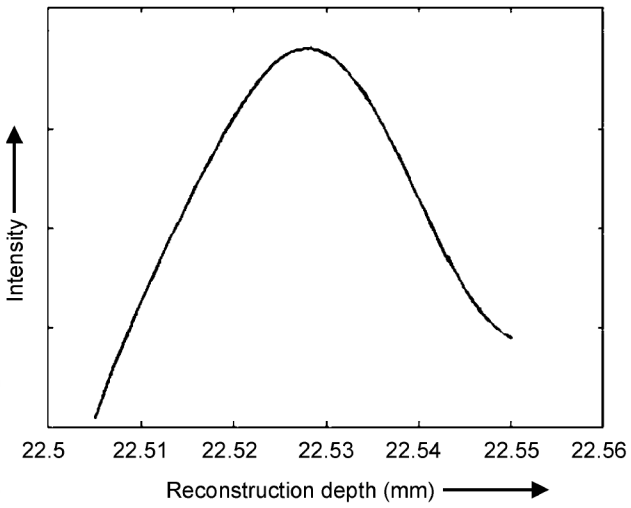

Figure 8. Average intensity of particle along reconstruction depth.

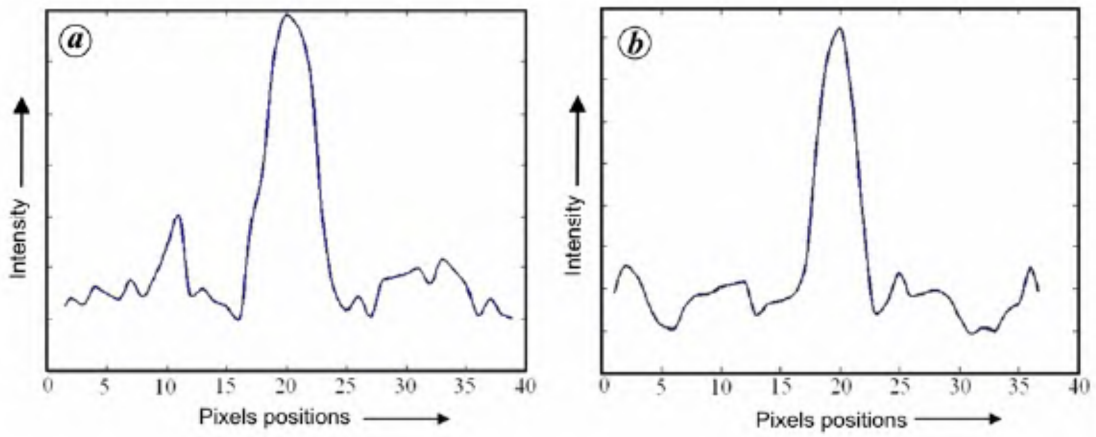

Figure 9. Intensity profile of the particle in Figure 7*a* along (***a***) *X*-direction and (***b***) *Y*-direction.

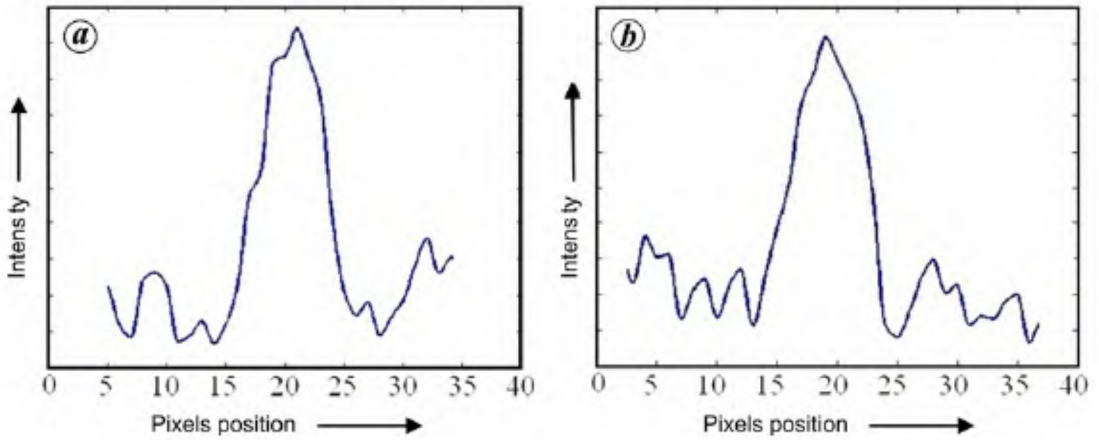

Figure 10. Intensity profile of particle 1 of Figure 7*b* along (***a***) *X*-direction and (***b***) *Y*-direction.

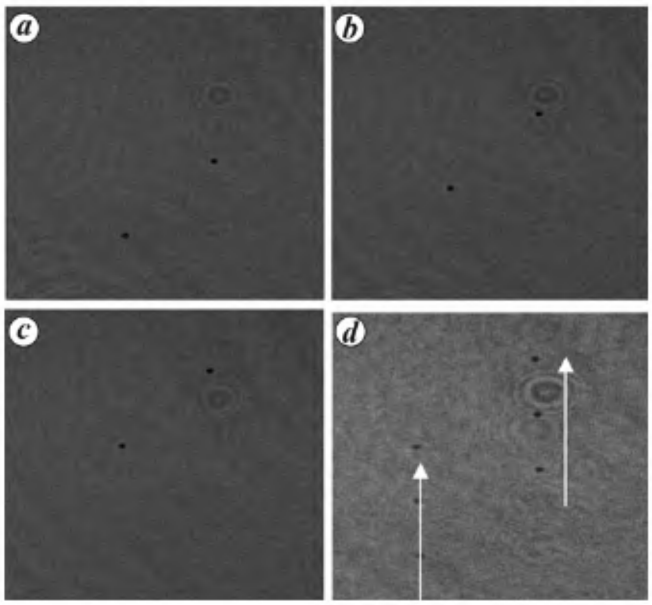

Figure 11. ***a***–***c***, Reconstruction of holograms of moving particles in a plane. ***d***, Addition of holograms prior to reconstruction provides motion in a single reconstruction frame.

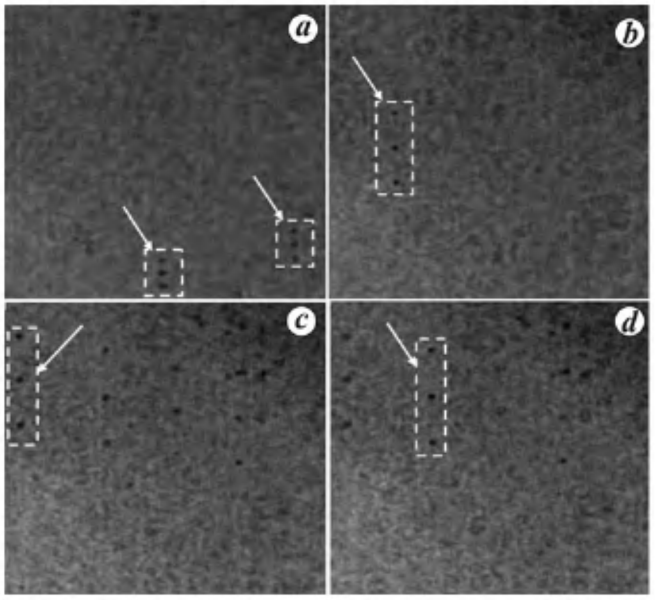

Figure 12. Analysis of dynamic particles by addition of holograms: (***a***) 19.43 mm, (***b***) 20.83 mm, (***c***) 21.45 mm and (***d***) 21.56 mm.

Addition of holograms prior to reconstruction can also provide the whole 3D field reconstruction of moving particles. This is also shown in Figure 12, where three holograms of the particle 3D distribution have recorded and added. The reconstruction in four different planes are shown in Figure 12 *a–d*, corresponding to the reconstruction distance 19.43 mm, 20.83, 21.45 and 21.56 mm respectively. The in-focus set of particles in the corresponding plane are highlighted. The displacement between the pixel positions of the particle can be used to study the velocity component in the corresponding plane. The displacement components in different planes show the flow behaviour of particles in different planes. The main disadvantage with the addition of hologram prior to reconstruction is the increase in noise in the reconstructed images. The noise level increases with increasing the number of holograms added. Thus for larger number of holograms or higher particle density, the noise increases significantly and thus a suitable numerical method has to be developed for the reduction of cumulative noise.

In conclusion, holograms of particles in different planes were digitally reconstructed using a single hologram. The method was extended to image the micro-particles along the depth of focus. This method is most effective for 3D particle analysis, particularly in flow fields because of the small depth of focus. For DH, the depth of focus depends on the particle size among other parameters, and hence this approach is best suited for the analysis of very small particles and low density in volume such as hypersonic shock tunnels. It has been shown that the digital holographic amplitude image of particles compares well with that of optical microscopic image. The LDHM system has been explored for its application in micro-particles analysis in 3D. Two methodologies have been developed for 3D dynamic analysis of micro-particles which can be used for particle size measurement, location with improved dynamic visualization and also for velocity measurements.

1. Gabor, D., Microscopy by reconstructed wavefronts. *Proc. Phys. Soc.*, 1951, **64**, 449–469.
2. Schnars, U. and Juptner, W. P. O., Digital recording and numerical reconstruction of holograms. *Meas. Sci. Technol.*, 2002, **13**, R85–R101.
3. Takaki, Y. and Ohzu, H., Fast numerical reconstruction technique for high-resolution hybrid holographic microscopy. *Appl. Opt.*, 1999, **38**, 2204–2211.
4. Ferraro, P., Coppola, G., Nicola, S. De, Finizio, A. and Pierattini, G., Digital holographic microscope with automatic focus tracking by detecting sample displacement in real time. *Opt. Lett.*, 2003, **28**, 1257–1259.
5. Grilli, S., Ferraro, P., Nicola, S. De., Finizio, A., Pierattini, G. and Meucci, R., Whole optical wavefields reconstruction by digital holography. *Opt. Express*, 2001, **9**, 294–302.
6. Kreis, T. M. Adams, M. and Juptner, W., Digital in-line holography in particle measurement. *Proc. SPIE*, 1999, **3744**, 54–64.
7. Javidi, B. and Tajahuerce, E., Three-dimensional object recognition by use of digital holography. *Opt. Lett.*, 2000, **25**, 610–612.
8. Xu, L., Peng, X., Asundi, A. and Miao, J., Hybrid holographic microscope for interferometric measurement of microstructures. *Opt. Eng.*, 2001, **40**, 2533–2539.
9. Coppola, G., Ferraro, P., Iodice, M., De Nicola, S., Finizio, A. and Grilli, S., A digital holographic microscope for complete characterization of microelectromechanical systems. *Meas. Sci. Technol.*, 2004, **15**, 529–539.
10. Singh, V. R., Miao, J., Wang, Z., Hegde, G. and Asundi, A., Dynamic characterization of MEMS diaphragm using time averaged in-line digital holography. *Opt. Commun.*, 2007, **280**, 285–290.
11. Pedrini, G., Fröning, P., Tiziani, H. and Santoyo, F., Shape measurement of microscopic structures using digital holograms. *Opt. Commun.*, 1999, **164**, 257–268.
12. Fournier, C., Barat, C., Ducttet, C. and Fournel, T., Digital holography applied to particle image velocimetry. Proc. PSFVIP-4, 2004, pp. 1–9.
13. Xu, W., Jericho, M. H., Meinertzhagen, I. A. and Kreuzer, H. J., Digital in-line holography for biological applications. *Proc. Natl. Acad. Sci. USA*, 2001, **98**, 11301–11305.
14. Kreis, T. M. and Juptner, W., Suppression of dc term in digital holography. *Opt. Eng.*, 1997, **36**, 2357–2360.
15. Takaki, Y., Kawai, H. and Ozhu, H., Hybrid holographic microscopy free of conjugate and zero-order images. *Appl. Opt.*, 1999, **38**, 4990–4996.
16. Pan, G. and Meng, H., Digital holography of particle fields: reconstruction by use of complex amplitude. *Appl. Opt.*, 2003, **42**, 827–833.
17. Fournier, C., Ducottet, C. and Fournel, T., Digital in-line holography: influence of the reconstruction function on the axial profile of a reconstructed particle image. *Meas. Sci. Technol.*, 2004, **15**, 686–693.
18. Fournier, C., Ducottet, C. and Fournel, T., Digital holographic particle image velocimetry: 3D velocity field extraction using correlation. *J. Flow Visual. Image Process.*, 2004, **11**, 1–20.
19. Virant, M. and Dracos, T., 3D PTV and its application on Lagrangian motion. *Meas. Sci. Technol.*, 1997, **8**, 1539–1552.
20. Pereira, F. and Gharib, M., Defocusing digital particle image velocimetry PIV and the three-dimensional characterization of two phase flows. *Meas. Sci. Technol.*, 2000, **13**, 683–694.
21. Ovryn, B., Three-dimensional forward scattering particle image velocimetry applied to a microscopic field-of-view. *Exp. Fluids*, 2000, **29**, S175–S184.
22. Pu, Y. and Meng, H., An advanced off-axis holographic particle image velocimetry HPIV system. *Exp. Fluids*, 2000, **29**, 184–197.
23. Bishop, A. I., Littleton, B. N., McIntyre, T. J. and Rubinstein-Dunlop, H., Near-resonant holographic interferometry of hypersonic flow. *Shock Waves*, 2001, **11**, 23–29.
24. McIntyre, T. J., Bishop, A. I., Eichmann, T. N. and Rubinsztein-Dunlop H., Enhanced flow visualization using near-resonant holographic interferometry. *Appl. Opt.*, 2003, **42**, 4445–4451.
25. Sucerquia, J. G., Xu, W., Jericho, S. K., Klages, P., Jericho, M. H. and Kreuzer, H. J., Digital in-line holographic microscopy. *Appl. Opt.*, 2006, **45**, 836–850.
26. Singh, V. R. and Asundi, A., Amplitude contrast image enhancement in digital holography for particles analysis. *Proc. SPIE*, 2005, **5878**, 58781–58787.
27. Repetto, L., Piano, E. and Pontiggia, C., Lensless digital holographic microscope with light-emitting diode illumination. *Opt. Lett.*, 2004, **29**, 1132–1135.
28. Pedrini, G. and Tiziani, H. J., Short-coherence digital microscopy by use of a lensless holographic imaging system. *Appl. Opt.*, 2002, **41**, 4489–4496.

Received 24 March 2008; revised accepted 18 December 2008